Association between the 11-Year Solar Cycle, the QBO, and the Atmosphere. Part II: Surface and 700 mb in the Northern Hemisphere in Winter

HARRY VAN LOON

National Center for Atmospheric Research, Boulder, Colorado*

KARIN LABITZKE**

Institut für Meteorologie, Freie Universität Berlin, Federal Republic of Germany

(Manuscript received 17 February 1988, in final form 11 May 1988)

ABSTRACT

Sea level pressure, surface air temperature, and 700-mb temperature and geopotential height show a probable association with the 11-year solar cycle which can be observed only if the data are divided according to the phase of the Quasi-Biennial Oscillation. The range of the response is as large as the interannual variability of the given element, and the correlations prove statistically meaningful when tested by Monte Carlo techniques. The sign of the correlations changes over the hemisphere on the spatial scale of extensive teleconnections. The correlations at 700 mb tend to be of opposite sign in the east and west years of the QBO, a result which Labitzke and van Loon also found in an analysis of the stratosphere. The pattern of correlation between the 700-mb heights on the Northern Hemisphere and the solar flux is the same as that of point-to-point correlations (teleconnections) between the 700-mb height at selected points and the heights at all other points. We interpret this similarity as a property of the atmosphere's internal dynamics, a favored resonance evoked within the atmosphere itself or by extraneous effects.

1. Introduction

This paper is part of an investigation of a recently discovered, likely association between the 11-year solar cycle and changes in the earth's atmosphere. A note on the discovery was published by Labitzke (1987), and a paper by Labitzke and van Loon (1988, hereafter referred to as LvL) described the solar relationship mainly in the lower and middle stratosphere.

The effect of the solar cycle can be detected only if the atmospheric data are divided according to the phase of the Quasi-Biennial Oscillation (QBO) in the zonal wind of the stratosphere above the equator. This circumstance limits the study to the last three and a half solar cycles, as the phase of the QBO cannot be defined before 1952 with our present knowledge. The idea to search for a solar–terrestrial relationship through the QBO stems from an observation by Labitzke (1982) that in the westerly phase of the QBO, major midwinter warmings (reversals) of the stratospheric polar vortex in the Northern Hemisphere tend to occur only in the maxima of the 11-year solar cycle.

* The National Center for Atmospheric Research is sponsored by the National Science Foundation.

** Visiting Scientist, National Center for Atmospheric Research.

Corresponding author address: Dr. Harry van Loon, NCAR, P.O. Box 3000, Boulder, CO 80307.

We observed in LvL that the stratospheric temperatures and geopotential heights in the west phase of the QBO are positively correlated with the solar cycle at higher latitudes and negatively correlated at middle and low latitudes; and conversely in the east phase of the QBO. Monte Carlo tests indicated that these results are unlikely due to sampling. Little or no association exists between complete time series of stratospheric temperatures and heights and the solar cycle because the correlation coefficients are inclined to change sign from the east to the west phase of the QBO.

2. Data sources and classification

We have used data from the following well-known sources:

1) U.S. National Meteorological Center: 700-mb geopotential heights and temperatures and sea level pressures at grid points.

2) Surface air temperatures and pressures from the Comprehensive Ocean Atmosphere Data Set (COADS).

3) Surface air temperature and sea level pressure at stations from the World Weather Records.

The winters were classified as being in the east or west phase of the QBO according to the wind direction in January at 50 and 40 mb: (50 + 40 mb)/2. The time

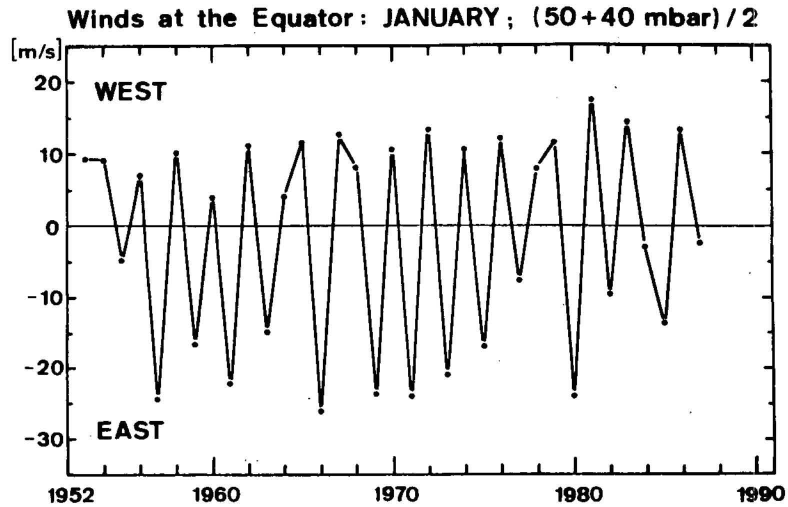

FIG. 1. Time series of the equatorial zonal wind (m s^{-1}) in January, (50 + 40 mb)/2. Based on Naujokat (1986, updated).

series in Fig. 1 shows the mean wind in January at these levels (updated from Naujokat 1986), and Table 1 lists the years in either phase as used here. One might be tempted to leave out 1 or 2 years which are on the borderline, but we have included all winters, and an inspection of Fig. 1 in Naujokat (1986) shows that they have this in common: in a winter classified as west, the mean vertical shear below 50–40 mb is westerly, and in one classified as east, the shear is easterly.

An additional reason for choosing the zonal wind at 50–40 mb for the classification may be seen in Fig. 2. This figure shows the correlation for (January + February)/2 between the 30-mb temperature at the North Pole and the 11-year solar cycle, with the winters classified according to the direction of the wind at five different levels above the equator. The correlation is highest when the direction of the 50–40 mb wind is used. Owing to the downward propagation of phase in the QBO, the correlation goes to zero between 30 and 20 mb, after which it increases with the opposite sign.

The statistical tests of our analyses are described in the Appendix. We note here only that the tests indicate

TABLE 1. Years (January and February) when the QBO was in the west or east phase.

West	East
1953	1952
1954	1955
1956	1957
1958	1959
1960	1961
1962	1963
1964	1966
1965	1969
1967	1971
1968	1973
1970	1975
1972	1977
1974	1980
1976	1982
1978	1984
1979	1985
1981	1987
1983	
1986	
$n = 19$	$n = 17$

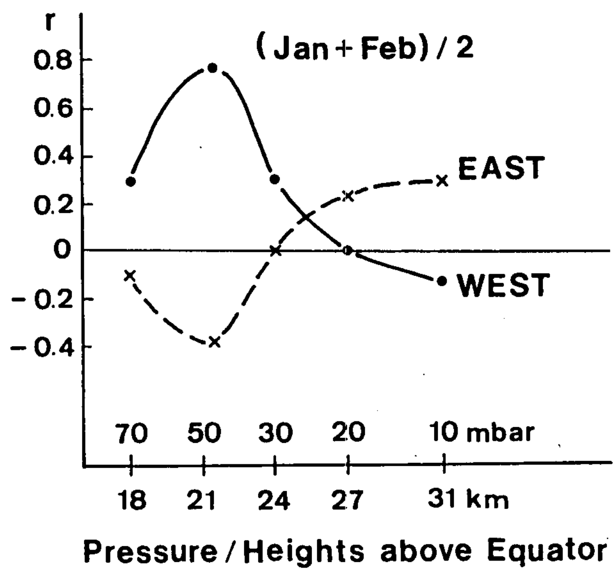

FIG. 2. Correlations between the 30-mb temperature in January–February at the North Pole and the 10.7 cm solar flux with the data stratified according to the zonal wind at different pressure levels above the equator. The mean of the 40 and 50 mb levels was used at the level marked 50 mb.

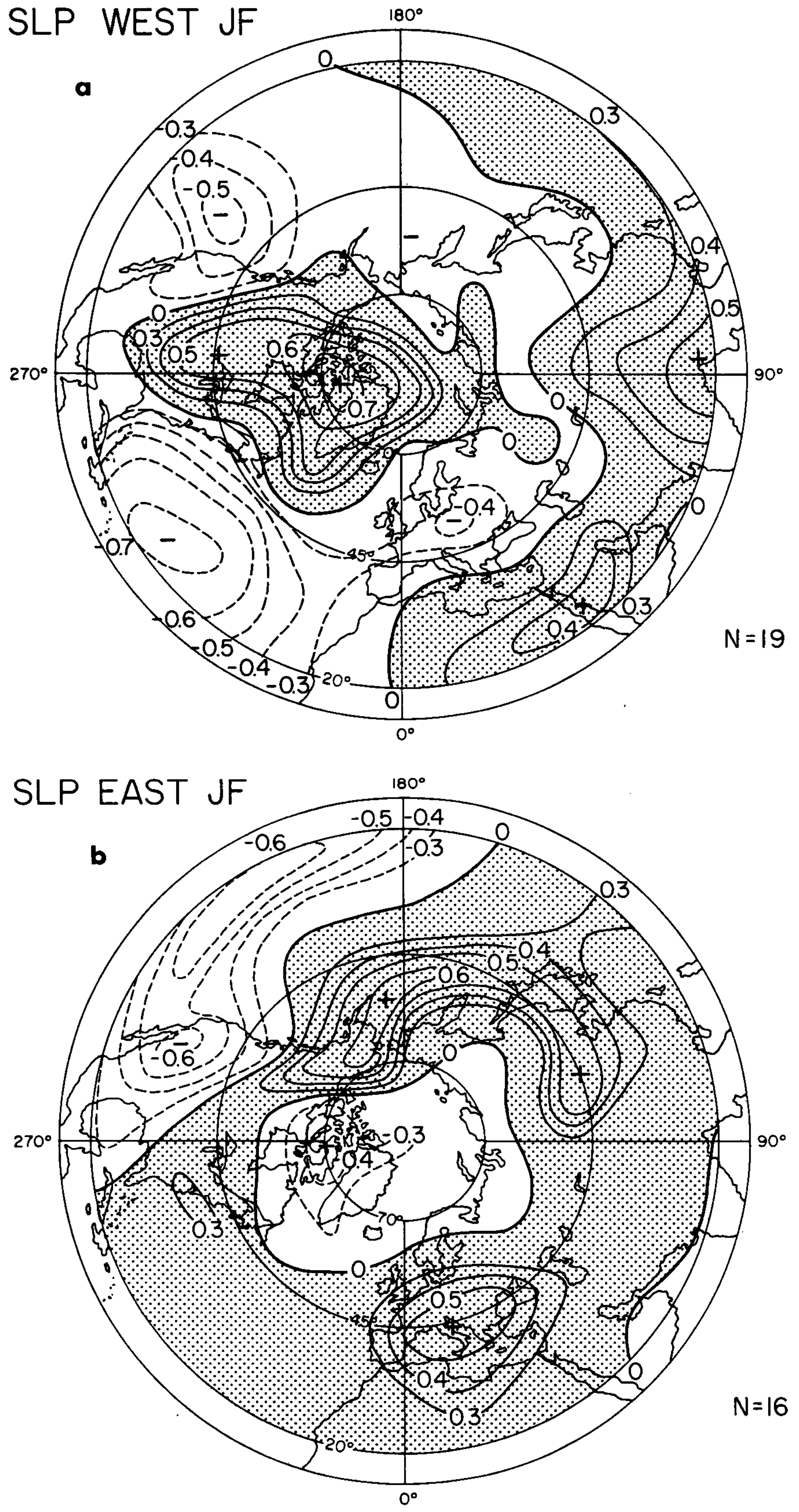

FIG. 3. Lines of equal correlation coefficient: sea level pressure in January–February at grid points correlated with the 10.7 cm solar flux for (a) 19 winters when the QBO was westerly and (b) 16 winters when the QBO was easterly.

TABLE 2. Positions of stations.

Akureyri	65.7°N, 18.1°W
Albuquerque	35.1°N, 106.6°W
Bergen	60.4°N, 5.3°E
Cape Hatteras	35.3°N, 75.6°W
Charleston, S.C.	32.9°N, 80°W
Des Moines	41.5°N, 93.7°W
El Paso	31.8°N, 106.4°W
McGrath	63°N, 155.6°W
Nashville	36.1°N, 86.7°W
The Pas	54°N, 101.1°W
Resolute	74.7°N, 95°W
Salt Lake City	40.8°N, 112°W

that the associations we find with the solar flux are not likely to be owing to chance.

3. Sea level pressure

It was noted in LvL that the marked response in the stratosphere to the variations in solar flux continues into the troposphere, and that the response is related to well-known teleconnection patterns. This section shows (Fig. 3a) the correlations between the solar flux and sea level pressure in 19 winters in the west phase, and the correlations in the 16 winters in the east phase (Fig. 3b). The overall patterns are discussed in section 5 together with the 700-mb correlation patterns. Here we give only some examples of how the correlation coefficients translate into time series and what the correlation patterns imply in terms of changes in horizontal pressure differences and anomalous winds.

Three stations have been chosen (positions in Table 2) in the area of positive correlation over North America to illustrate the relationship between the solar flux and the pressure in the west phase (Fig. 4). Two of them, Des Moines and The Pas, lie where the correlation coefficient is between 0.5 and 0.6, and the third, Resolute, where the correlation is 0.7. In all three instances the association between the two curves is conspicuous as the extremes of pressure tend to occur in extremes of the solar cycle. The signal is also large *and covers the whole interannual variability* of the mean January–February sea level pressure, with 15 mb at Resolute and The Pas and 9 mb at Des Moines. Two stations in the east phase from a region with negative correlations about −0.6, Albuquerque and El Paso in Fig. 5, have the same close relationship with the solar cycle, and the variability covers the whole interannual range.

Because the correlations change sign on the scale of planetary waves, correlations between the solar cycle and zonal averages of pressure, or averages over large regions, lead to insignificantly small numbers.

In a solar *maximum* the pressure tends to be high over North America in the west phase of the QBO (Fig. 3a), and low over the adjacent oceans. The anomalous wind then has a northerly component between the center of the continent and the Atlantic Ocean, and a southerly component over the western half of the continent. In a solar *minimum* during the west phase, the anomalous wind tends to be southerly over the eastern half of North America, and northerly over the western half. These conditions are illustrated by the time series in Fig. 6. The series in Fig. 6a is for the point 70°N, 100°W where the correlation coefficient is 0.72. The series for 20°N, 60°W in Fig. 6b with a correlation of −0.70 represents the negative area in the North Atlantic. The difference between the two in Fig. 6c is proportional to the anomalous geostrophic wind which thus has a close association with the solar cycle during

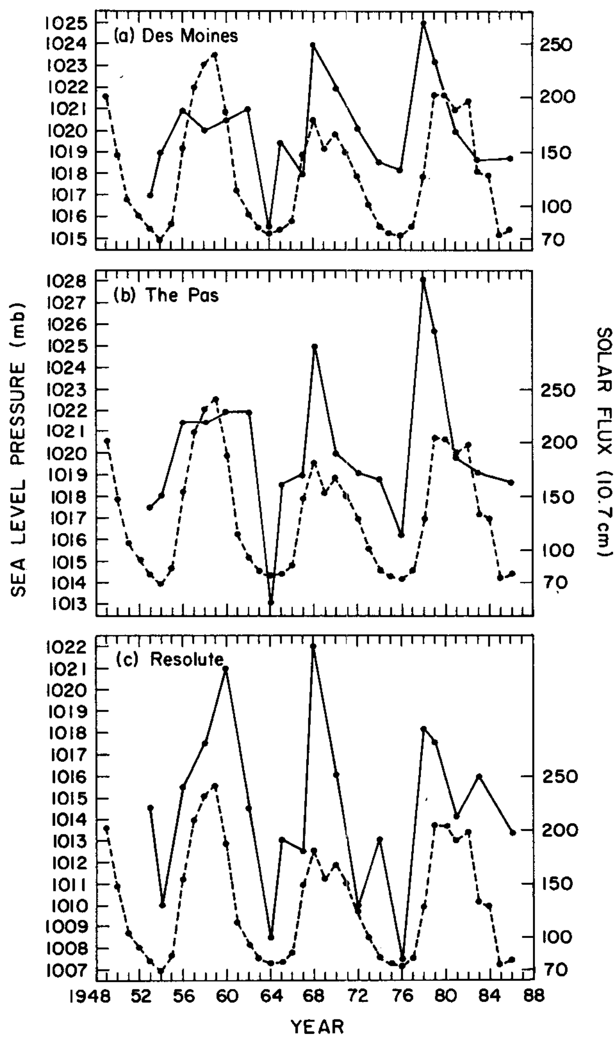

FIG. 4. Time series of the 10.7 cm solar flux for all years (dashed line) and of sea level pressure at three North American stations (position in Table 2) for the years when the QBO was westerly in January–February.

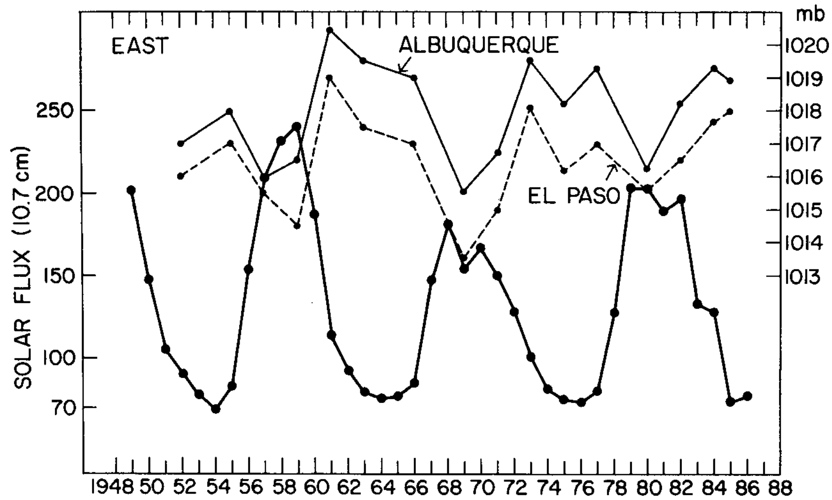

FIG. 5. As in Fig. 4 except for two stations in years when the QBO was easterly.

the 19 winters. The pressure differences between the two points have a range of 15 mb, which is close to the total interannual variability.

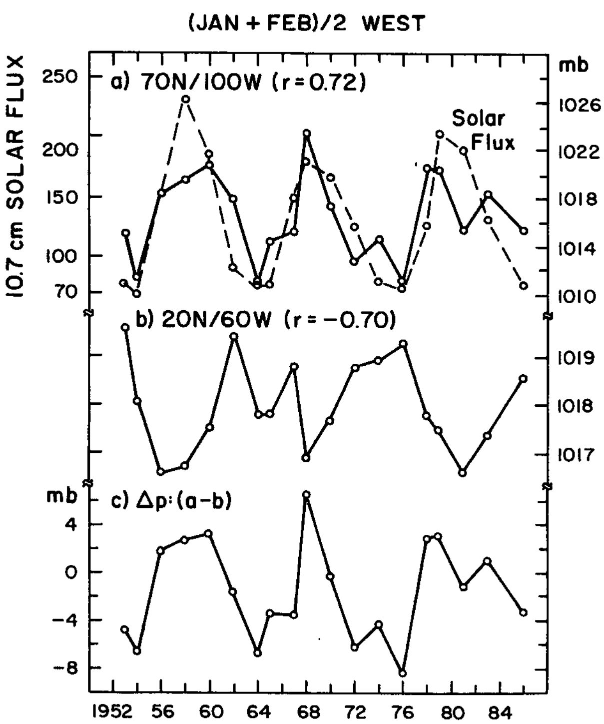

FIG. 6. Time series in January–February for 19 years when the QBO was westerly of (a) 10.7 cm solar flux (dashed line) and the sea level pressure at 70°N, 100°W; (b) the sea level pressure at 20°N, 60°W; (c) the difference in sea level pressure (a) − (b). The correlation coefficients are correlations with the solar flux.

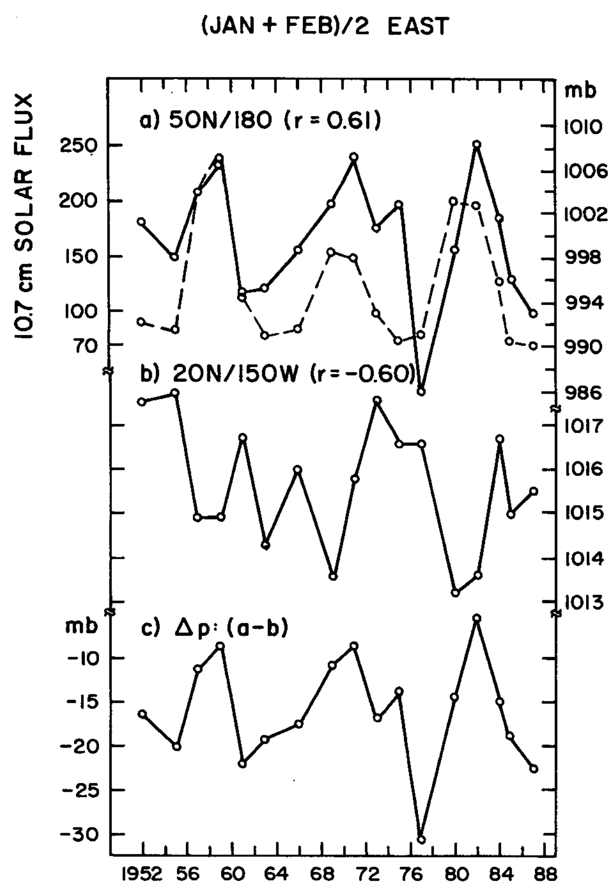

FIG. 7. Time series in January–February for 17 years when the QBO was easterly of (a) 10.7 cm solar flux (dashed line) and the sea level pressure at 50°N, 180°W; (b) the sea level pressure at 20°N, 150°W; (c) the difference in sea level pressure (a) − (b). The correlation coefficients are correlations with the solar flux.

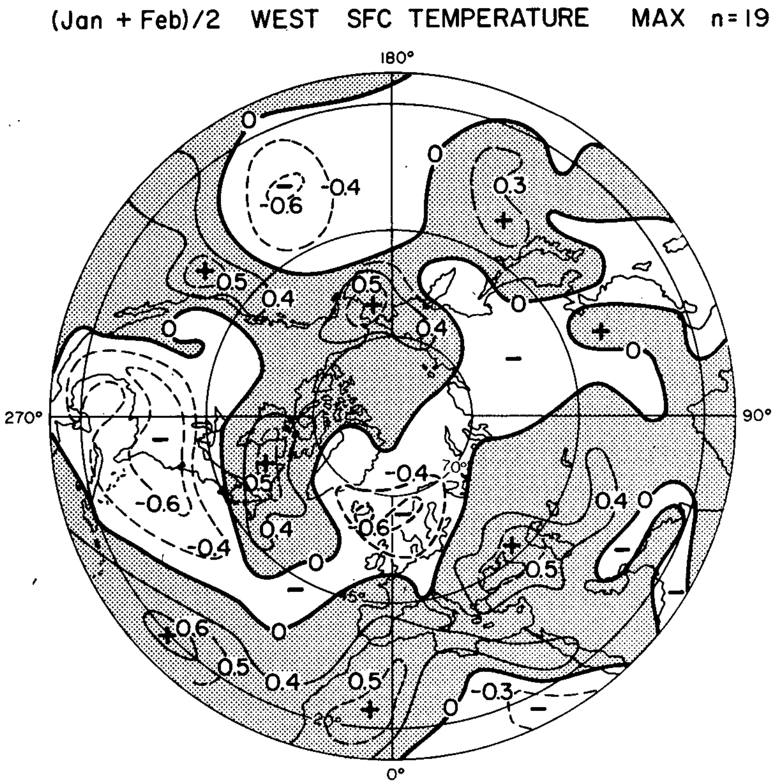

FIG. 8. Lines of equal correlation coefficient: surface air temperature in January–February in west years at stations and in COADS blocks correlated with the 10.7 cm solar flux. Largest possible sample for land stations is 19 years, and for COADS blocks 16 years.

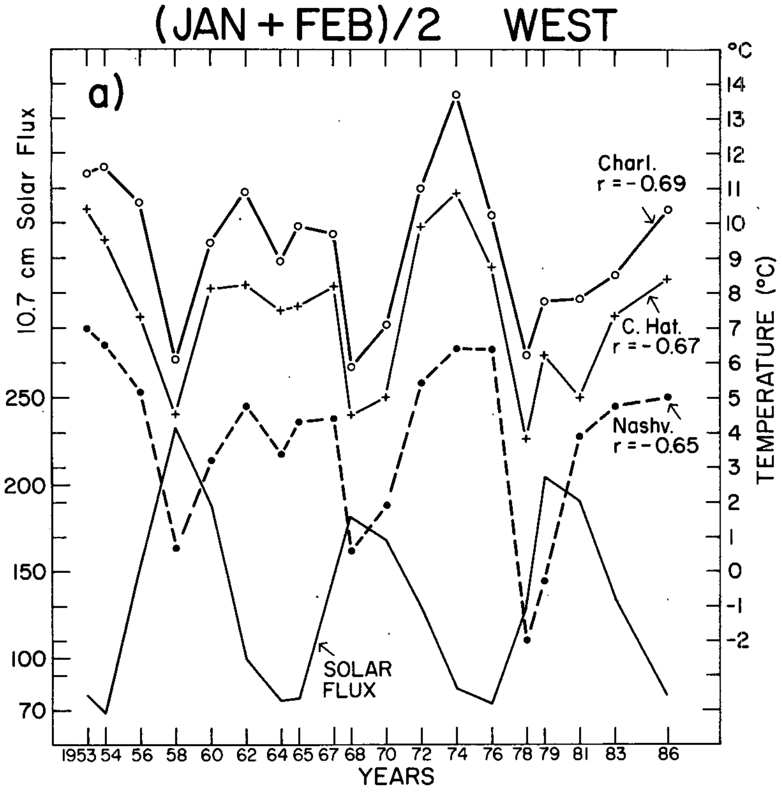

FIG. 9. Time series for January–February in the west years of the QBO of the 10.7 cm solar flux and of surface air temperature at (a) three United States stations (positions in Table 2), (b) two North Atlantic stations, and (c) an Alaskan station. The correlation coefficients are for temperature correlated with the flux.

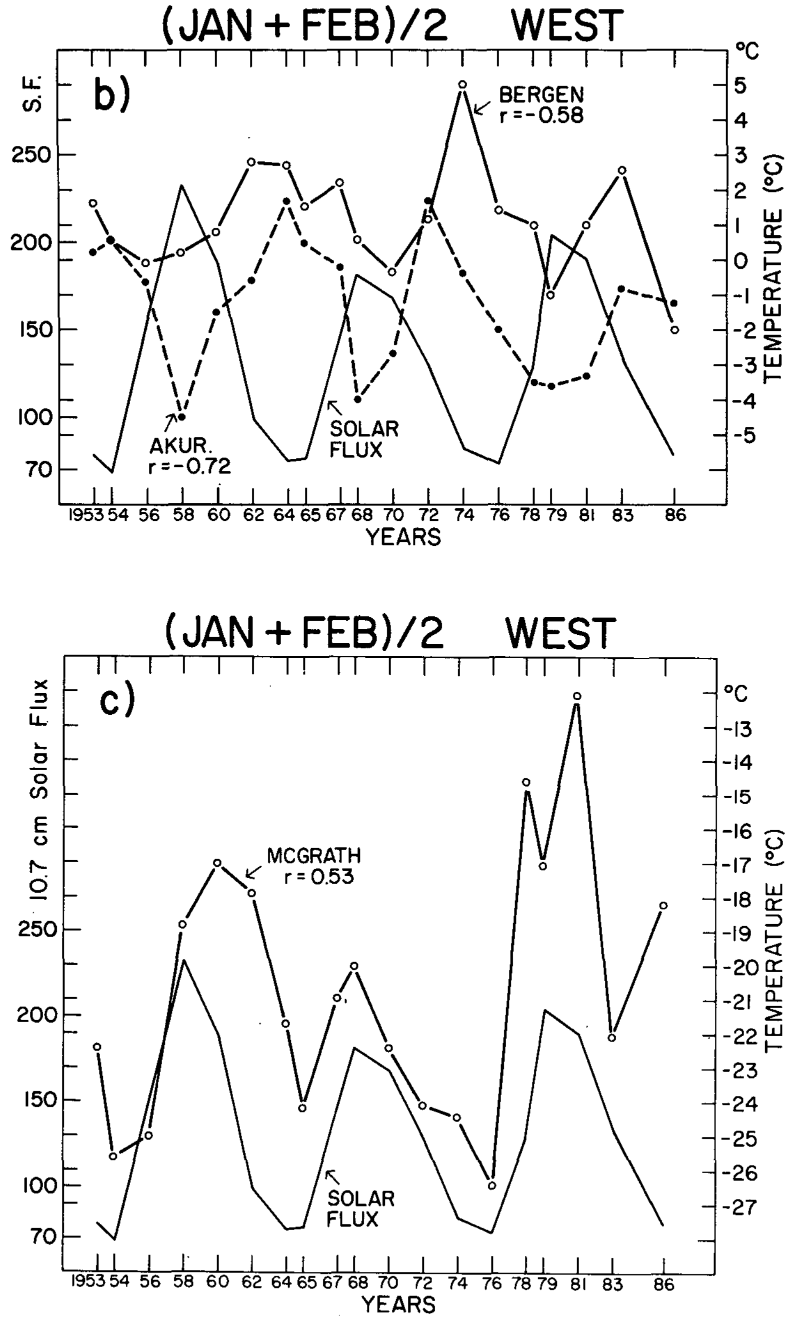

FIG. 9. (*Continued*)

Similar series for the east phase of the QBO are shown in Fig. 7 for the points at 50°N, 180° ($r = 0.61$) and 20°N, 150°W ($r = 0.60$). The difference between them is in Fig. 7c. Over the Pacific Ocean the association in this phase of the QBO is such that in a solar maximum the pressure tends to be above normal over the northern part of the ocean (Fig. 7a) and below normal over the southern part (Fig. 7b), with reduced westerlies between the two areas (Fig. 7c). In a solar minimum the anomalies are negative in the north and positive in the south, and the westerlies are enhanced.

4. Surface air temperature

Anomalous winds such as those described above are associated with simultaneous temperature anomalies (van Loon and Williams 1976, 1977). This effect is illustrated in the map (Fig. 8) of the correlations between surface air temperatures in the west years of the QBO and the solar flux in the same years. We used all available stations for this purpose and the COADS was used over the oceans. The largest possible sample for the stations is 19 years, and for the COADS 16 years.

We note a few features in Fig. 8. The anticyclonic anomalous circulation in solar maxima, indicated by the positive pressure correlations over North America in Fig. 3a, is associated with negative temperature correlations over the Norwegian Sea (northeasterly anomalous wind); positive temperature correlations over Labrador (easterly anomalous wind); negative temperature correlations over the southwest Atlantic and the central eastern United States (northeasterly wind); and positive temperature correlations from the waters off California to Alaska (southerly anomalous wind). Between 90°W and 45°E the correlation pattern in Fig. 8 has many features in common with the temperature pattern connected with the North Atlantic seesaw (van Loon and Rogers 1978).

Figure 9 shows time series of the temperatures in the west years and of the solar flux in the same years. The stations lie near the largest correlation coefficients of each area and all are well related to the solar cycle, inversely in the United States and at Akureyri and Bergen (Fig. 9a, b), and directly at McGrath (Fig. 9c).

A comparison between the pressure correlations in Fig. 3b and the temperature correlations in Fig. 10 shows the association between the solar cycle and pressure (wind) and temperature in the east phase of the QBO. For instance, in solar maxima there is an anomalous cyclonic circulation over the Pacific south of 45°N ($r < 0$), and in solar minima an anomalous anticyclonic circulation. In the solar maxima the temperature therefore tends to be lower than in solar minima in the south central part of the ocean (northeasterly anomalous wind). In the eastern part and over the Rocky Mountains the temperature would be higher in the solar maxima than in the minima (southerly anomalous wind). The two time series in Fig. 11 of the mean January–February temperature at stations in the western United States illustrate the association with the solar cycle in the east phase.

In the east phase the main signal in the pressure is in an area centered on the Pacific Ocean, whereas in the west phase little goes on in the Pacific in comparison with North America and the Atlantic region (cf. Figs. 3a, b). The temperature signals show similar differences with respect to the two regions.

5. 700-mb geopotential heights and temperature

The correlations between the 700-mb geopotential height and the solar flux in the west years of the QBO (Fig. 12a) have the same general pattern as the correlations with sea level pressure in Fig. 3a. An interesting implication of the correlations is that the westerlies across North America into the Atlantic Ocean quite often must be appreciably weaker in solar maxima than in solar minima when the QBO is westerly, whereas the opposite holds from North Africa to central Russia. The pattern in the east years (Fig. 12b) also reflects that at the surface (Fig. 3b). In this phase, too, there are obvious implications for the wind. For example, the westerlies in the Pacific Ocean would be weaker in solar maximum than in solar minimum.

In many respects Figs. 12a and 12b are opposites; e.g., the area with negative correlations from Mexico to northern Europe in the west years has a counterpart in the positive correlations over the same area in the east years. A similar opposition of sign exists from North Africa to southern Asia. This tendency for reversal of sign from east to west years, which was found in the stratosphere as well (LvL), is even more marked in the 700-mb temperature (Figs. 13a, b), which means that the pattern in solar maxima in the east years resembles the one in solar minima in the west years, and vice versa.

We pointed out in LvL that the occurrence of major midwinter warmings (breakdowns) of the polar vortex in the stratosphere often is linked to the phase of the QBO in conjunction with the state of the solar cycle: in the west years the warmings tend to occur in solar maxima, and in the east years during solar minima. The anomalous patterns at 700 mb associated with these warmings may be gleaned from Figs. 12 and 13. High pressure over Labrador–Baffin Island with low pressure in the subtropics of the Atlantic Ocean, for instance, would be associated with the stratospheric warmings during the west phase of the QBO in solar maxima (Fig. 12a). In the east phase the warmings would tend to occur in solar minima with anomalously low pressure near the Aleutians and high pressure to the south (Fig. 12b). The stratospheric warmings in the west phase are associated with an anomaly pattern in the 700-mb temperature of the same sign as the correlations in Fig. 13a. In the east phase the 700-mb temperature anomalies associated with major warmings in the stratosphere would have the opposite sign of the correlations in Fig. 13b.

The patterns of correlation of 700-mb geopotential height with the solar cycle in Fig. 12 are the same as well-known teleconnection patterns. With the permission of Jerome Namias we show two teleconnection maps for December–January–February from his *CALCOFI Atlas* (1981) in Fig. 14. In Fig. 14a the 700-mb height for 1948–72 at the point 70°N, 90°W, where r is big in Fig. 12a, is correlated with the 700-mb heights elsewhere on the hemisphere. *The configuration of these point-to-point correlations is to all practical purposes the same as those obtained by correlating all points with the solar flux in the west phase* (cf. Fig. 12a).

In the east phase, Namias's correlations based on 30°N, 50°E (Fig. 14b) may be compared with our Fig.

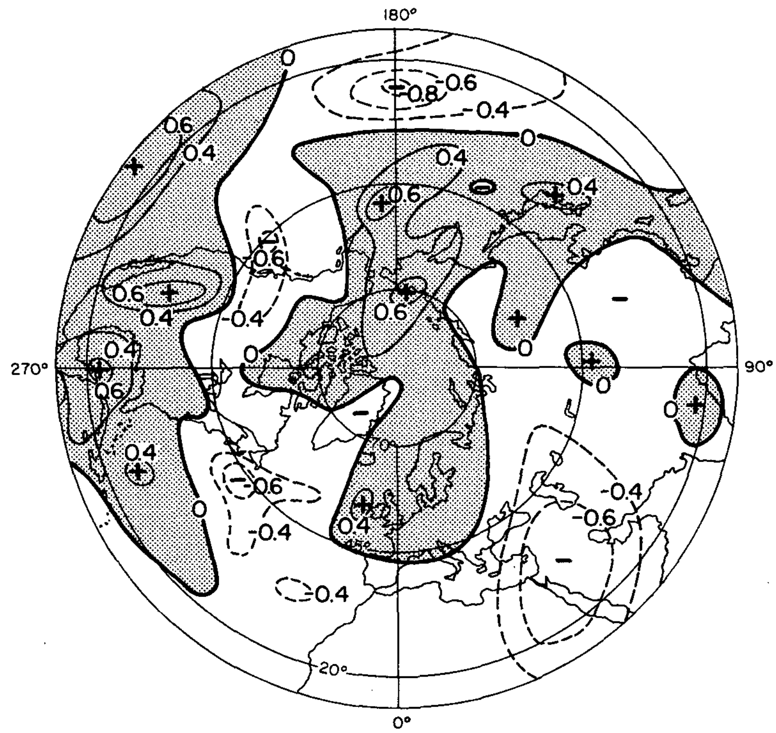

FIG. 10. As in Fig. 8 except for years when the QBO was easterly. Maximum number in a sample is 16 years.

12b where this point has the highest correlation with the solar cycle. As in the west phase, the correlation with the solar cycle shows in essence the same design as Namias's point correlations.

Namias's maps are for the whole winter (DJF) and cover the years 1948–72. We have repeated his point correlations (Fig. 15) for all January–February months from 1952 to 1986, the period covered by our solar

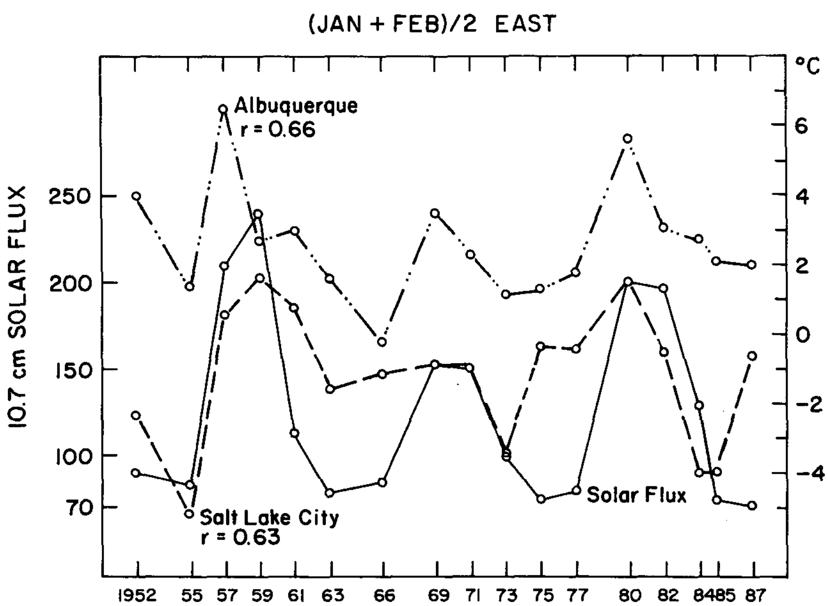

FIG. 11. As in Fig. 9 except for two United States stations in years when the QBO was easterly.

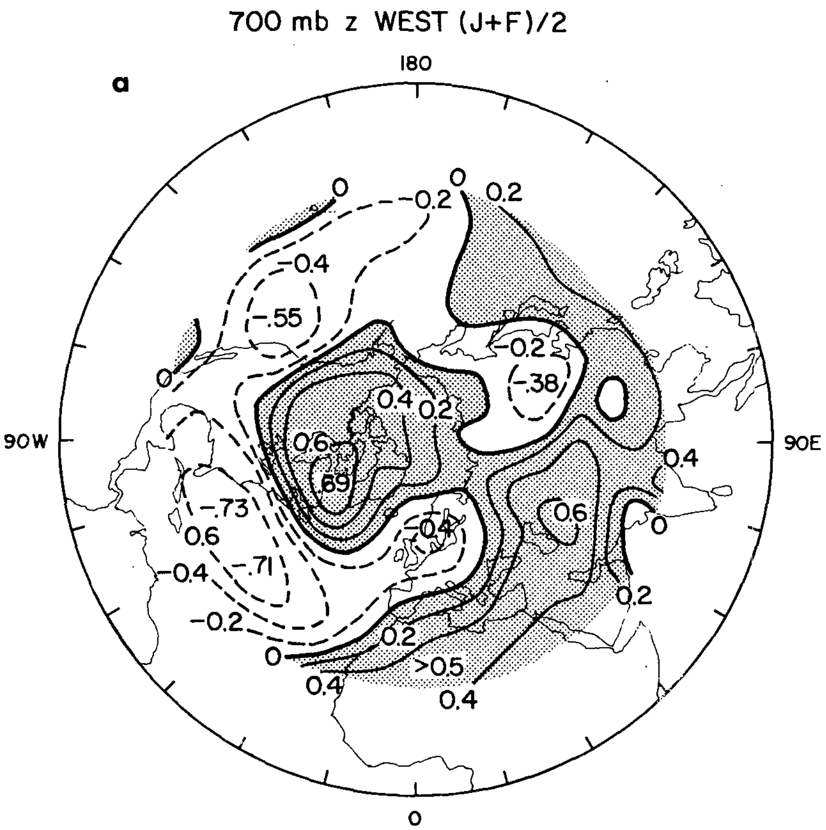

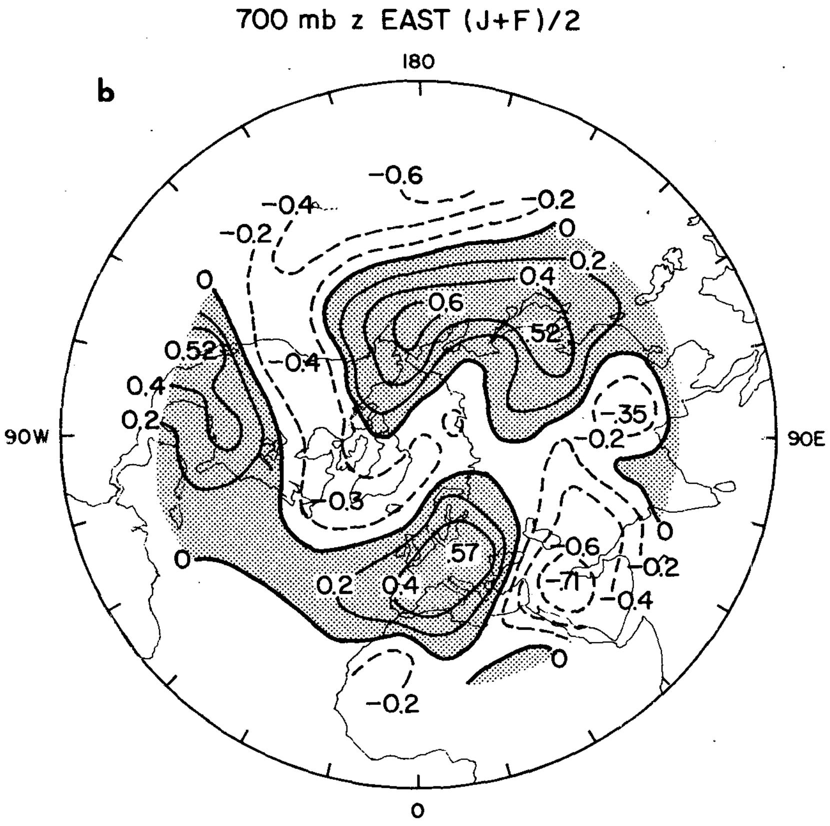

FIG. 12. Lines of equal correlation between 700-mb geopotential height at grid points and the 10.7 cm solar flux, in January–February and for years of (a) westerly and (b) easterly QBO.

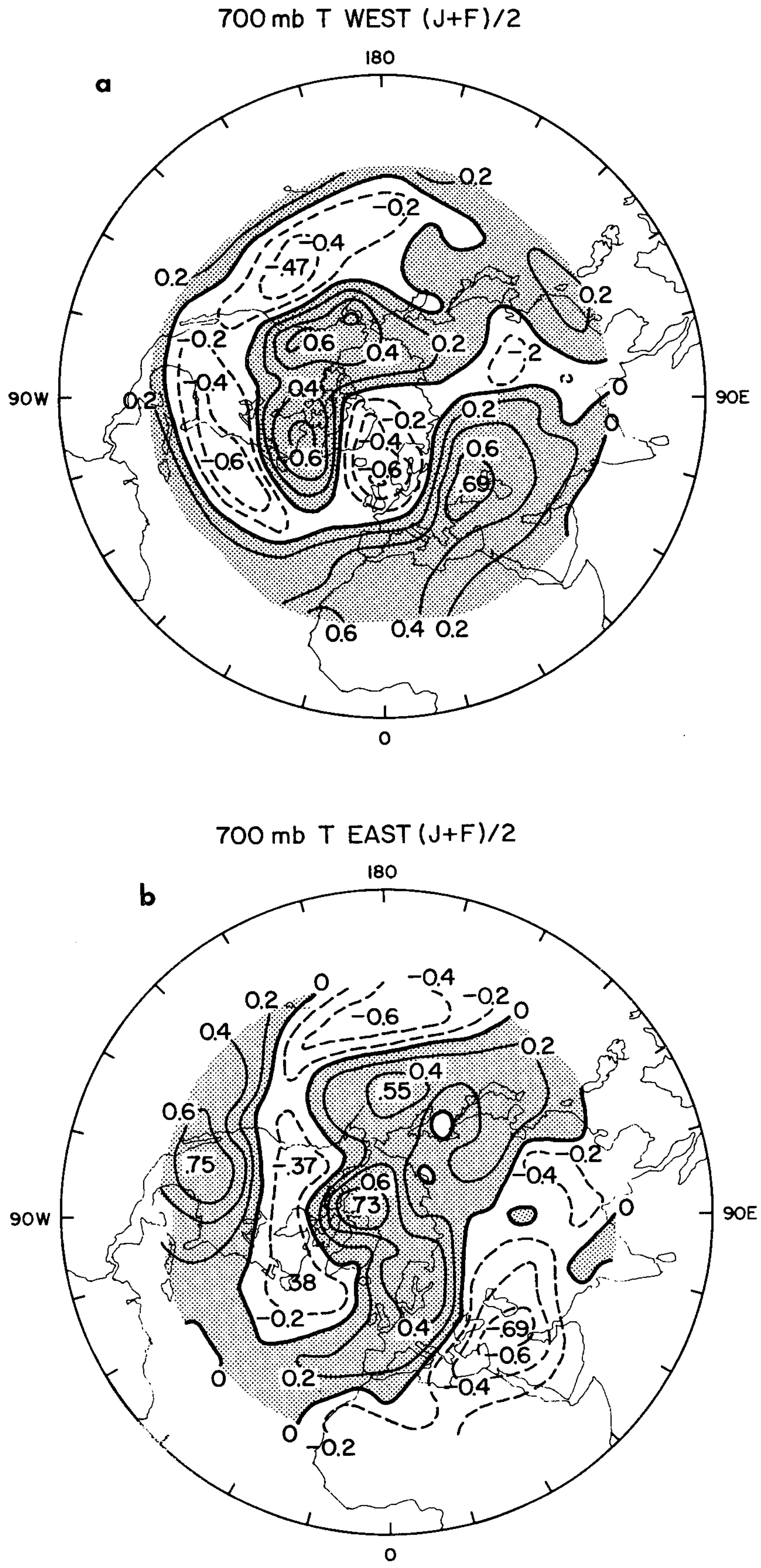

FIG. 13. As in Fig. 12 except for 700-mb temperature.

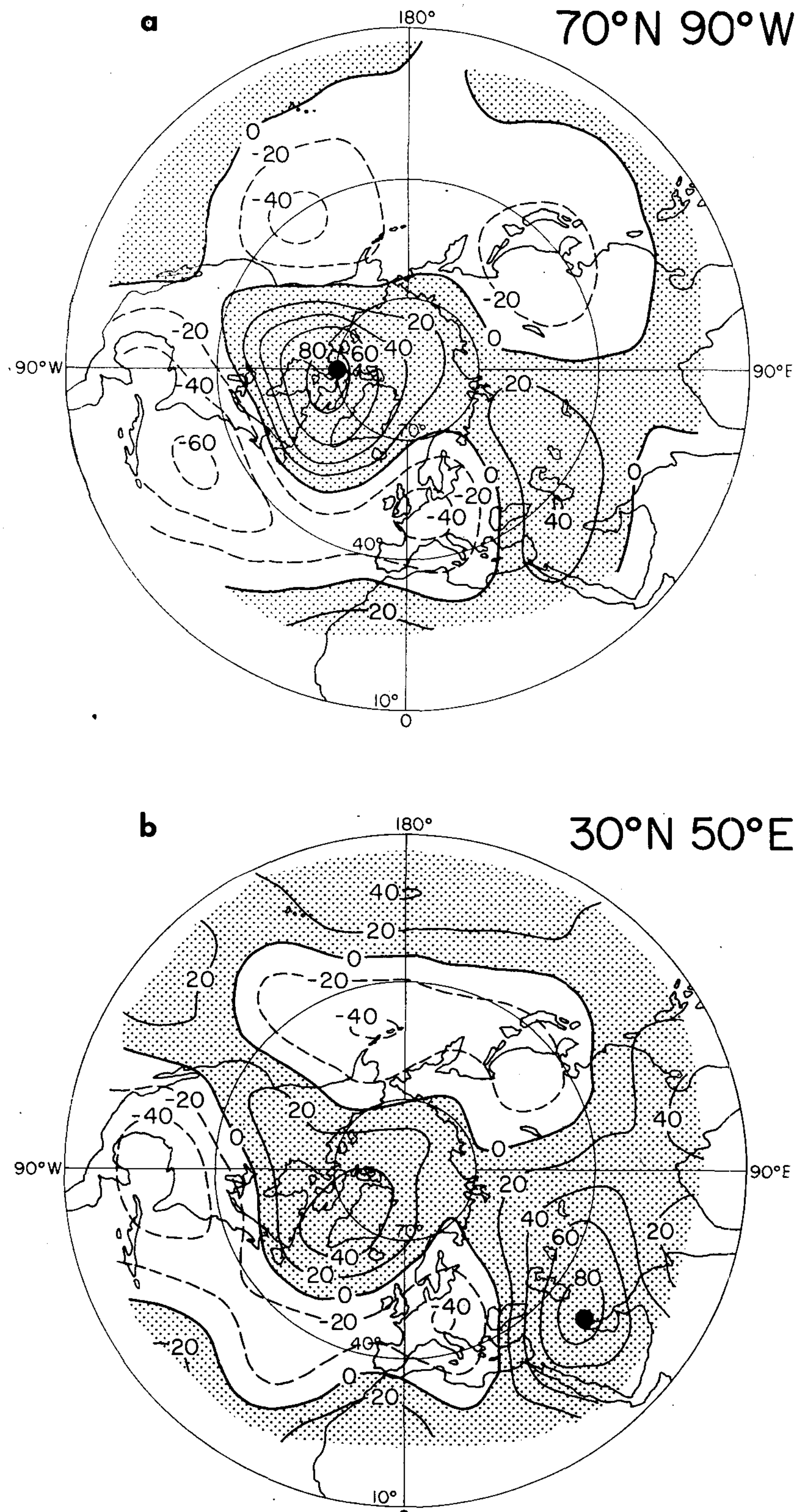

FIG. 14. Lines of equal correlation between the 700-mb geopotential height at (a) 70°N, 90°W or (b) 30°N, 50°E and the 700-mb height elsewhere, for December–January–February and 1948–72. From Namias (1981), reproduced with the kind permission of J. Namias.

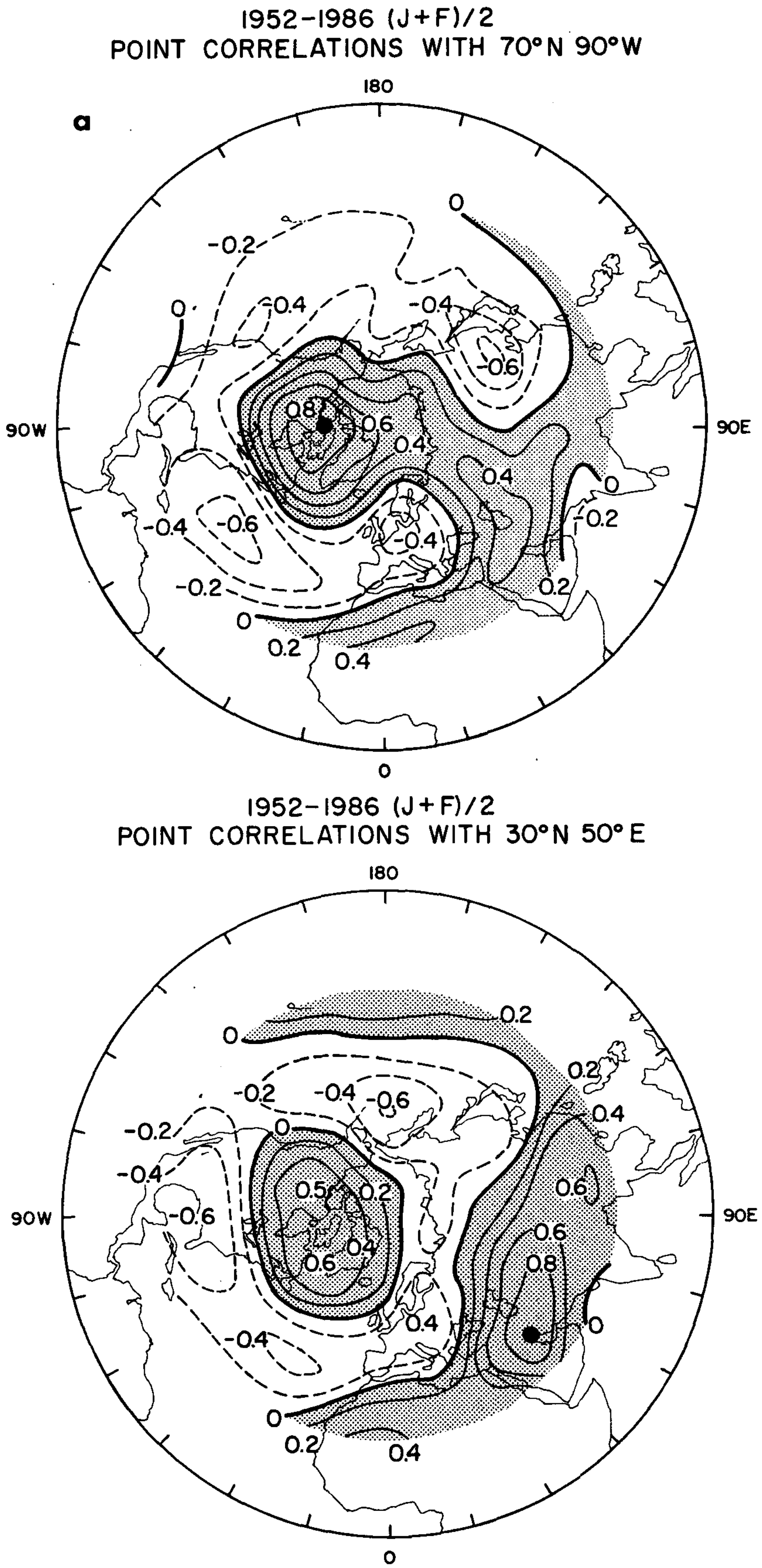

FIG. 15. Lines of equal correlation between the 700-mb geopotential height at (a) 70°N, 90°W or (b) 30°N, 50°E and the 700-mb height elsewhere, for January–February and all years between 1952–86.

flux correlations in Fig. 12. The patterns in the two types of correlations, point-with-point and with the solar flux, are again remarkably similar, especially in the west years. In the east years (Fig. 12b), the sign is the opposite of that in the point correlations, as the point 30°N, 50°E was selected because of its large correlation (negative) with the solar flux; in Fig. 15b it is correlated with all other points.

The fact that correlation of 700-mb height with the solar flux yields the same pattern as that produced when the 700-mb height at selected points is correlated with the heights over the whole hemisphere, does not immediately lead to an understanding of *where* and *how* the solar variability might excite the atmosphere. Such a pattern may be regarded as an attribute of the atmosphere's internal dynamics, a favored resonance which is evoked within the atmosphere itself or when it is exposed to extraneous influences. On the other hand, as the atmosphere responds readily in this mode, the forcing may not have to be especially large.

6. Conclusion

When the data on the Northern Hemisphere (sea level pressure, surface air temperature, and 700-mb temperature and geopotential heights) in January–February are grouped according to the direction of the zonal wind at 50–40 mb above the equator (the Quasi-Biennial Oscillation) and correlated with the 10.7 cm solar flux, surprisingly large correlation coefficients result. The range of the atmospheric elements in this association is as large as that of their interannual variability. The sign of the correlation is not uniform over the hemisphere but changes on the scale of extensive teleconnections. There is a marked tendency for the correlation patterns at 700 mb to be opposites in the east and west years of the QBO which was also observed in the stratosphere (LvL).

If points of large correlation between 700-mb heights and the solar flux are used as central points for correlation with the 700-mb heights at all other points, the design of the point-to-point correlations is similar to that of correlations between the 700-mb height at all points and the 11-year solar cycle. Interesting as this is, it does not immediately explain where and how solar variability might excite the atmosphere. It is likely that the similarity between the response to the solar flux and the point-to-point correlations within the atmosphere reflects a favored resonance of the atmosphere, inherent in its internal dynamics.

We can investigate only three and a half solar cycles owing to the limitations imposed by our dependence on the QBO. Despite the internal consistency of our analyses and the favorable results of rigorous statistical testing, one cannot exclude the possibility that our results are not generally valid. We cannot explain how the known solar variability could produce such large responses in the northern winter. Some of our colleagues have suggested that what we have detected is a strong tendency for large-amplitude atmospheric variability on a decadal time scale which shows when the observations are filtered through the Quasi-Biennial Oscillation. This is of course a possibility, but such variability has no obvious explanation either. We find it remarkable if an internal oscillation in the atmosphere on a decadal time scale happened to be in phase with the 11-year solar cycle during the very 36 years when we describe it.

Acknowledgments. We are deeply indebted to Dennis J. Shea for designing and performing the statistical tests. We have benefitted from frequent, enlightening discussions with D. Shea, D. Baumhefner, G. Branstator, and J. Tribbia.

APPENDIX

Estimates of Statistical Significance

The maps of correlation between the 10.7 cm solar flux and sea level pressure and 700-mb temperature and geopotential heights are based on grid-point values with 19 winters in the west years and 16 in the east years. The maps (Figs. 8, 10) showing the correlations with surface air temperature were analyzed by means of data from land stations and COADS, and the lines of equal correlation coefficients on these two maps are drawn conservatively because the coefficients are not based on the same length of record. In the west years the largest possible sample is 19 years for land stations and 16 years for COADS blocks; in the east years it is 16 years for land stations and 12 years for COADS. The correlations are tested by the bootstrap technique, using the observations near the centers of largest correlation coefficients.

The bootstrap technique—a Monte Carlo method—works in the following way (Efron 1982). At Charleston the correlation coefficient between temperature in January–February and the 10.7 cm solar flux for 19 winters in the west years is −0.69. Is this correlation close to the true value of r for all correlations between Charleston's temperature in January–February and the solar flux? First, each of the observed 19 pairs of temperature and solar flux is copied 10 000 times, and all 190 000 pairs are mixed thoroughly. Then 1000 "bootstrap samples" of 19 pairs each are picked at random from the 190 000 pairs and the correlation coefficient is computed for each of these 1000 samples. In our bootstrap samples 95% of the correlation coefficients at Charleston fall between −0.46 and −0.83; only 5% are larger than −0.83 or smaller than −0.46. Half of the width of this interval can be interpreted as the

TABLE 3. Bootstrap test of surface air temperatures, and the interval which contains 95% of the correlations in the bootstrap sample of 1000.

Position	Name	*n*	*r*	Interval with 95% of correlations
		West		
65.8°N, 24.2°E	Haparanda	19	−0.56	−0.27–−0.73
60.1°N, 1.2°W	Lerwick	19	−0.61	−0.29–−0.77
65.7°N, 18.1°W	Akureyri	18	−0.72	−0.41–−0.86
39.9°N, 41.3°E	Erzurum	18	0.54	0.20–0.75
44.1°N, 43.0°E	Pjatigorsk	18	0.58	0.20–0.80
13.8°N, 13.7°W	Tambcounda	19	0.59	0.31–0.76
22.9°N, 42.9°W	COADS	16	0.66	0.30–0.91
12.9°N, 63.0°W	COADS	16	0.72	0.43–0.84
32.9°N, 80.0°W	Charleston	19	−0.69	−0.46–−0.83
36.1°N, 86.7°W	Nashville	19	−0.65	−0.33–−0.86
36.9°N, 69.0°W	COADS	16	−0.75	−0.53–−0.86
64.2°N, 83.4°W	Coral Harbour	19	0.48	0.13–0.69
52.8°N, 51.0°W	COADS	14	0.57	0.18–0.81
63.0°N, 155.6°W	McGrath	19	0.53	0.18–0.75
37.0°N, 132.9°W	COADS	16	0.71	0.34–0.86
37.0°N, 154.9°W	COADS	16	−0.60	−0.28–−0.76
		East		
32.0°N, 34.9°E	Lod	16	−0.66	−0.23–−0.87
39.9°N, 41.3°E	Erzurum	16	−0.64	−0.34–−0.80
15.6°N, 32.6°E	Khartoum	15	−0.64	−0.17–−0.86
55.0°N, 16.9°W	COADS	12	0.74	0.40–0.89
42.8°N, 54.9°W	COADS	12	−0.69	−0.30–−0.91
21.1°N, 86.5°W	COADS	12	0.70	0.27–0.87
35.1°N, 106.6°W	Albuquerque	16	0.66	0.36–0.86
47.0°N, 132.9°W	COADS	11	−0.60	−0.28–−0.78
18.8°N, 125.0°W	COADS	12	0.72	0.19–0.88
24.9°N, 179.0°W	COADS	12	−0.83	−0.44–−0.93
51.0°N, 172.9°W	COADS	11	0.71	0.26–0.87
34.9°N, 144.9°E	COADS	12	0.59	0.23–0.82

bootstrap estimate of the average amount by which the observed value of *r* for a random sample of 19 differs from the true value of *r*. The true value could be anywhere between −0.5 and −0.9, but it is almost certainly not zero.

Table 3 shows the correlation coefficients in the west and east years, the size of the sample, and the width of the interval within which lie 95% of the correlations in the bootstrap sample of 1000. In the best instance (COADS, 36.9°N, 69°W, $r = -0.75$ and the 95% interval between −0.53 and −0.86) the average distance from the true value is 0.165. In the worst (COADS, 18.8°N, 125°W, $r = 0.72$ and the 95% interval between 0.19 and 0.88) the average distance is 0.345. Similar examples can be gathered from Tables 4–6. Nearly all

TABLE 4. Bootstrap test of sea level pressure, and the interval which contains 95% of the correlations in the bootstrap sample of 1000.

Position	Name	*n*	*r*	Interval with 95% of correlations
		West		
74.7°N, 95.0°W	Resolute	19	0.69	0.47–0.81
54.0°N, 101.1°W	The Pas	19	0.59	0.30–0.82
46.8°N, 100.8°W	Bismarck	19	0.59	0.28–0.81
25.0°N, 55.0°W	COADS	16	−0.75	−0.45–−0.90
33.2°N, 133.0°W	COADS	16	−0.60	−0.24–−0.81
		East		
43.1°N, 141.3°E	Sapporo	16	0.56	0.15–0.78
55.2°N, 162.7°W	Cold Bay	16	0.59	0.32–0.79
35.1°N, 106.6°W	Albuquerque	16	−0.64	−0.38–−0.79
47.0°N, 168.9°W	COADS	12	0.64	0.19–0.83
20.8°N, 138.9°W	COADS	12	−0.66	−0.25–−0.92

TABLE 5. Bootstrap test of 700-mb geopotential height, and the interval which contains 95% of the correlations in the bootstrap sample of 1000.

Position	*r*	Interval with 95% of correlations
	West (19 years)	
20°N, 0°	0.58	0.24–0.76
40°N, 60°E	0.63	0.25–0.81
25°N, 75°W	−0.73	−0.48–−0.86
60°N, 60°W	0.69	0.45–0.81
60°N, 115°W	0.59	0.29–0.82
35°N, 130°W	−0.55	−0.25–−0.79
	East (16 years)	
30°N, 45°E	−0.71	−0.42–−0.88
55°N, 25°E	0.57	0.31–0.75
40°N, 135°E	0.56	0.13–0.83
50°N, 175°E	0.66	0.40–0.81
20°N, 175°E	0.66	−0.43–−0.84
20°N, 110°W	−0.53	0.19–0.76

TABLE 6. Bootstrap test of 700-mb temperature, and the interval which contains 95% of the correlations in the bootstrap sample of 1000.

Position	*r*	Interval with 95% of correlations
	West (19 years)	
20°N, 15°W	0.66	0.40–0.80
45°N, 40°E	0.69	0.38–0.83
60°N, 0°	−0.62	−0.30–−0.82
60°N, 60°W	0.64	0.32–0.82
60°N, 160°W	0.62	0.17–0.84
35°N, 140°W	−0.47	−0.11–−0.73
30°N, 60°W	−0.63	−0.35–−0.78
	East (16 years)	
35°N, 50°E	−0.69	−0.45–−0.85
65°N, 10°E	0.53	0.19–0.84
75°N, 110°W	0.73	0.40–0.85
50°N, 175°E	0.55	0.17–0.79
25°N, 175°E	−0.63	−0.32–−0.83
30°N, 105°W	0.75	0.55–0.90

of the tests indicate that it is unlikely that the true correlations in the selected points were zero or of the opposite sign.

REFERENCES

Efron, B., 1982: *The Jackknife, the Bootstrap and Other Resampling Plans.* Soc. Industr. Appl. Math., Philadelphia, J. W. Arrowsmith, Bristol, England, 92 pp.

Labitzke, K., 1982: On the interannual variability of the middle stratosphere during northern winters. *J. Meteor. Soc. Japan,* **60,** 124–139.

——, 1987: Sunspots, the QBO, and the stratospheric temperature in the north polar region. *Geophys. Res. Lett.,* **14,** 535–537.

——, and H. van Loon, 1988: Association between the 11-year solar cycle, the QBO, and the atmosphere. Part I: The troposphere and stratosphere on the Northern Hemisphere in winter. *J. Atmos. Terres. Phys.,* in press.

Namias, J., 1981: Teleconnections of 700 mb height anomalies for the Northern Hemisphere. *CALCOFI Atlas No. 29,* A. Fleminger, Ed., Marine Life Research Program, Scripps Institution of Oceanography, I–VII + 265 pp.

Naujokat, B., 1986: An update of the observed Quasi-Biennial Oscillation of the stratospheric winds over the tropics. *J. Atmos. Sci.,* **43,** 1873–1877.

van Loon, H., and J. Williams, 1976: The connection between trends of mean temperature and circulation at the surface. Part I: Winter. *Mon. Wea. Rev.,* **104,** 365–380.

——, and ——, 1977: The connection between trends of mean temperature and circulation at the surface. Part IV: Comparison of the surface changes in the Northern Hemisphere with the upper air and with the Antarctic in winter. *Mon. Wea. Rev.,* **105,** 636–647.

——, and J. C. Rogers, 1978: The seesaw in winter temperatures between Greenland and northern Europe. Part I: General description. *Mon. Wea. Rev.,* **106,** 295–310.